Crowding effects on the small, fast-folding protein λ$_{6\text{-}85}$

Sharlene Denos[a], **Apratim Dhar**[b], and **Martin Gruebele**[a,b,c]

Martin Gruebele: mgruebel@illinois.edu

[a]Center for Biophysics and Computational Biology, 600 South Mathews Avenue, University of Illinois, Urbana-Champaign, IL 61801

[b]Department of Chemistry, 600 South Mathews Avenue, University of Illinois, Urbana-Champaign, IL 61801

[c]Department of Physics, 600 South Mathews Avenue, University of Illinois, Urbana-Champaign, IL 61801

Abstract

The microsecond folder λ$_{6\text{-}85}$ is a small (9.2 kDa = 9200 amu) five helix bundle protein. We investigated the stability of λ$_{6\text{-}85}$ in two different low-fluorescence crowding matrices: the large 70 kDa carbohydrate Ficoll 70, and the small 14 kDa thermophilic protein SubL. The same thermal stability of secondary structure was measured by circular dichroism in aqueous buffer, and at a crowding fraction φ=15±1% of Ficoll 70. Tryptophan fluorescence detection (probing a tertiary contact) yielded the same thermal stability in Ficoll, but 4 °C lower in aqueous buffer. Temperature-jump kinetics revealed that the relaxation rate, corrected for bulk viscosity, was very similar in Ficoll and in aqueous buffer. Thus viscosity, hydrodynamics and crowding seem to compensate one another. However, a new fast phase was observed in Ficoll, attributed to a lower activation barrier and downhill folding. We also measured the stability of λ$_{6\text{-}85}$ in φ=14±1% SubL, which acts as a smaller more rigid crowder. Significantly greater stabilization (7 to 13 °C depending on probe) was observed than in the Ficoll matrix. The results highlight the importance of crowding agent choice for studies of small, fast-folding proteins amenable to comparison with molecular dynamics simulations.

1. Introduction

Unimolecular reactions of small molecules in the aqueous phase usually have a fairly straightforward dependence on solvent condition, given by Kramers' model.[1] What about large unimolecular reactants, such as a protein folding to its native state? When large proteins are crowded in aqueous solution by other large molecules (e.g. high molecular weight carbohydrates), interesting things can happen. For example, the reaction can speed up upon crowding, even though the viscosity increases[2] (and the reaction is not in the Kramers anomalous regime). But when is a protein really a 'large' molecule? In recent years, the fast folding kinetics of many 'small' (20–100 amino acid) proteins has been studied, and the results now can be compared directly with full atom molecular dynamics simulations.[3] Until now, the folding kinetics of such 'small' proteins has not been examined in crowding environments.

When proteins fold, they traverse an energy landscape that can be characterized overall by two parameters: its energetic bias towards the native state, and its energy roughness.[4] If we perform the Legendre transform from energy to free energy (relevant in the laboratory where

Correspondence to: Martin Gruebele, mgruebel@illinois.edu.

temperature, not entropy, is the adjustable parameter) a continuous range of scenarios emerges. At one extreme, if the bias is weak and the roughness is large, folding intermediates accumulate. This is the likely scenario for large proteins with many opportunities for non-native contacts. Work on smaller proteins has demonstrated that folding intermediates are not obligatory for folding: small proteins usually fold over a single barrier,[5] analogous to most chemical reactions.[6] Going even further to the other extreme, the native bias can become so large, and the roughness so small that some small proteins fold without any significant barrier at all, analogous to many ion-molecule, excited electronic state, or radical reactions.[7] Extensive experimental and computational evidence for downhill folding in solution has been accumulated in recent years.[8–24]

Downhill folding can be detected thermodynamically:[9] When there is a substantial barrier to heat-induced unfolding, a single melting (unfolding) temperature T_m is obtained by all spectroscopic probes. Without such a barrier, tuning the temperature yields different T_m for different probes.[9, 15, 19] Downhill folding can also be detected dynamically (Figure 1A): When there is a substantial barrier, a single activated rate coefficient k_a for folding is measured. Upon lowering the barrier, k_a at first simply increases; but when the population diffusing through the transition state reaches a detectable size, the rate coefficient becomes time-dependent at short times.[11] In this limit, reaction kinetics becomes reaction dynamics. The time it takes for the rate coefficient to settle into a constant plateau value k_a is termed 'molecular rate' or $k_m = \tau_m^{-1} \gg k_a$.[6] It can be measured to extract absolute folding barriers $G^\dagger$ directly from experiment:[11]

$$\Delta G^\dagger = k_B T \ln(k_m / k_a) \quad [1]$$

Because of large protein size and solvent viscosity, k_m is much greater for proteins (typically > 100 ns) than for small molecule reactions (typically < 1 ps).

Very recently, single trajectory molecular dynamics simulations on the Anton supercomputer have confirmed downhill folding of small proteins in solution computationally via observation of repeated folding and unfolding events.[3] Sampling was sufficient to compute one dimensional potentials of mean force (PMFs, coordinate-dependent free energies) using Hummer's coordinate reduction method.[25] For example, Anton simulations and thermodynamic experiments agree that a certain protein BBL mutant has a negligible activation barrier even at T_m.[3, 13] For the largest protein folded by a single trajectory to date (Figure 1B), a mutant of the 5 helix bundle λ_{6-85}, experiment yielded an absolute barrier of ≈4kJ/mole at 65 °C,[11] and a melting point range of T_m = 68 °C (fluorescence detection) to 73.5 °C (circular dichroism detection). The Anton simulation yielded an identical barrier height of ≈4kJ/mole at 77 °C. There is good reason to believe that globular protein domains (usually < 200 amino acids) will be foldable in solution routinely by single trajectory,[26] multi-trajectory[27] or replica[21] molecular dynamics techniques to Ångstrom accuracy within a decade, as calibration against experiments further improves the accuracy of empirical force fields, yielding better stabilities, kinetic mechanisms, and structures.[28]

As a result, experimental work to study protein folding in more realistic environments has accelerated during the past several years. Proteins are now studied on the ribosome,[29, 30] in densely packed crowding agents,[31–37] and even in living cells directly.[38, 39] Significant changes of protein stability and folding kinetics are expected in such complex environments, based on the aqueous solution results outlined above: free energy barriers and stabilities of proteins are small (10s of kJ/mole), and thus easily modulated by interactions of the protein with its solvation environment. For technical reasons, crowding studies have focused on

large proteins so far; no experimental results are available for small sub-millisecond folders suitable for all atom simulation, the closest being the small heme protein cytochrome c that folds in under a second.[40]

Here we study λ_{6-85}, already discussed above, in two very different crowding environments: Ficoll 70, a 70 kDa semi-rigid cross-linked carbohydrate that acts as a roughly spherical crowder in aqueous solution; and SubL, a 14 kDa thermophilic protein that serves as a smaller and more rigid crowder than the commonly used large molecular weight carbohydrates (Figure 1C). We find that the stability of λ_{6-85} in Ficoll deviates only little from aqueous solution. A small probe dependence of the melting temperature in aqueous buffer (circular dichroism *vs.* fluorescence) disappears in Ficoll. T-jump kinetics of λ_{6-85} in Ficoll likewise reveals similar rates in Ficoll as in aqueous buffer, although a molecular phase 'burst' precedes the activated unimolecular kinetics in Ficoll 70. To enhance crowding effects, we propose the new protein crowder SubL.[41] It is smaller and more rigid than Ficoll, thermophilic ($T_m > 90$ °C), and has very low fluorescence, making it an ideal match for crowding small, fast-folding proteins such as λ_{6-85} by fluorescence techniques. We find that SubL has a larger effect on λ_{6-85} stability at volume fractions comparable to those for Ficoll. We conclude that SubL matrices provide a better size match and more rigid crowding environment for small, fast folding proteins such as lambda repressor fragments.

2. Methods

2.1 Sample preparation

The fluorescent lambda repressor fragment λ^*_{6-85} ($T_m = 61°C$ by circular dichroism$=$CD[42]) and its Glu33Tyr/Ala37,49Gly mutant λ^*_{6-85}YG ($T_m = 54.5°C$ by CD[42]) were expressed and purified as described previously.[42] A tyrosine 22 to tryptophan mutation makes both proteins strongly fluorescent when excited at 290 nm.[43] λ^*_{6-85}YG tryptophan fluorescence monitors a specific Trp22-Tyr33 tertiary interaction[23] whose thermodynamics and kinetics we studied in Ficoll, while λ^*_{6-85} has a strongly decreasing fluorescence upon unfolding, ideally suited for studies in the slightly fluorescent SubL crowder.

A pET-19b plasmid containing the gene for protein SubL from the thermophile *Methanococcus jannashii* (obtained from Prof. Gary Olsen) was transformed and expressed in BL21(DE3) Rosetta cells. Protein was harvested by French Press and purified by heating to 62 °C to precipitate non-thermophilic cell lysate, followed by column chromatography. The chromatography protocol consisted of Ni-NTA affinity purification followed by size exclusion purification and a second Ni-NTA affinity purification. The His purification tag was not removed and the resulting protein had a mass of 14028 Da. Purified protein was dialyzed against double deionized water and checked for purity by MALDI and ESI mass spectrometry prior to lyophilization.

λ^*_{6-85}YG crowded by Ficoll 70 was prepared by mixing concentrated protein buffers with carbohydrate buffers (50 mM NaH$_2$PO$_4$, pH 7.0). Volume fractions in the range 15±1% Ficoll (240 mg/ml[44]) were used. λ^*_{6-85} samples crowded by SubL were prepared by adding lyophilized protein to 2 mL of buffer (300 mM NaCl, 50 mM NaH$_2$PO$_4$, pH 7.0), and then concentrating 4 times in <200 mTorr vacuum overnight. The buffer had no effect on SubL stability below 90 °C. A crowding fraction of $\varphi = 14\pm1\%$ SubL (220 mg/ml) was used for SubL. These crowding fractions avoided precipitation of the protein in the matrices.

Final concentration of lambda repressor in the matrices were determined using UV/Visible absorption at 280 nm and an extinction coefficient of 1750 M^{-1}cm^{-1} for SubL, 6970 M^{-1}cm^{-1} for λ_{6-85} mutants and $\approx$0 for Ficoll. The lambda repressor concentrations in the

matrix were kept at least 10 times lower than the matrix concentration to avoid strong interaction of lambda repressor with itself.

2.2 Circular dichroism and fluorescence measurements

Samples were overlaid with mineral oil to prevent evaporation. Larger temperature steps and minimal collection time for acceptable signal-to-noise ratio were used to reduce sample denaturation at higher temperatures.

Fluorescence spectra of lambda repressor, in aqueous buffer, crowded by Ficoll, or crowded by SubL, were measured as a function of temperature using a Varian (Palo Alto, CA) Cary Eclipse spectrofluorimeter with a 4-position Peltier multicell changer and a PCB-150 circulating water bath. Emission spectra were obtained from 300 to 400 nm upon 290 nm excitation of the tryptophan 22 residue, using slit widths of 5 nm for both emission and excitation monochromators to maximize signal. Temperature titrations were performed using a nitrogen purge of the sample chamber and the temperature probe placed directly in the buffer blank cuvette.

For Ficoll crowding only, it was also possible to measure circular dichroism spectra and melts of lambda repressor on a JASCO J-715 spectropolarimeter equipped with a Peltuer temperature controller. We simultaneously collected total fluorescence intensity (320–450 nm) during hose scans. No CD melts could be obtained for lambda repressor in the SubL matrix because SubL itself has a large CD spectrum and is at much higher concentration than the probe protein.

CD thermal melts dilute SubL solutions, to measure its stability, were obtained on a JASCO J-715 spectropolarimeter. The samples were 5 μM SubL in 2 M GuHCl denaturant at pH 4.5, and 264 mg/ml SubL in 2 M NaCl, 200 mM NaH$_2$PO$_4$ buffer at pH 7.

Integrated fluorescence and CD data were normalized and plotted as a function of temperature. We used a simple cooperative thermodynamic model to obtain T_m by fitting fluorescence and CD intensities. Table 1 summarizes the results of the model fits. The cooperative model is

$$[N] = \frac{K_{eq}}{1+K_{eq}} = 1 - [D], \quad K_{eq} = e^{-\Delta G(T)/RT}, \quad \Delta G(T) = C^{(1)}(T - T_m) \quad [2]$$

In this expression, [N] and [D] are the native and denatured concentrations as detected by either intensity or wavelength shift, K_{eq} is the folding equilibrium constant, $G(T)$ is the folding free energy as a function of temperature. We approximate it here by a just the linear Taylor series expansion, which was sufficient to fit all the data: $C^{(1)}$ measures how quickly the population switches from native to denatured state at T_m. (A heat capacity-based model from ref. 45 provides equally satisfactory fits.)

2.3 Temperature-jump kinetics in Ficoll

We measured T-jump kinetics of λ^*_{6-85} YG crowded by Ficoll 70 under the same buffer conditions used to measure stability. The experiment has been described in detail before.[46] Briefly, a train of 280 nm UV pulses from a frequency-tripled, mode-locked Ti:S laser is used to excite the sample tryptophan fluorescence in a 0.025 diameter by 0.4 mm long sample region every 12.5 ns. A 10 °C T-jump is then induced in the sample by a Raman-shifted (1.9 μm) Nd:YAG laser collimated at the sample to a ~ 1 mm diameter spot. The change in tryptophan fluorescence lifetime is recorded as folding kinetics progress, and plotted as " " normalized from 1 (just after the jump) to 0 (500 μs after the jump). λ^*_{6-85} YG

relaxes in *ca.* 50 μs, significantly slower than the <5 μs relaxation rates observed for the fastest downhill-folding mutants of lambda repressor.[15, 23] Thus we use the two-state approximation $k_a \approx k_{obs} K_{eq}/(1+K_{eq})$ to determine the activated folding rate coefficient from the observed rate coefficient k_{obs} and folding equilibrium constant K_{eq} (determined from fluorescence measurements in 2.2). The molecular phase k_m (downhill folding) and activated phase k_a have been discussed extensively elsewhere,[11, 15, 23, 47] and here we plot only k_a to see if the crowder has an effect on the small folding barrier.

To correct folding rates for bulk solvent viscosity, we measured the viscosity of Ficoll solutions with a Bohlin Instruments High Resolution C-VOR Torque Rebalance in viscometry mode, using a double gap couette cell, steel solvent trap and a Polyscience recirculating water bath. Measurements were performed at 20, 45, 48, 50, 53, 55, 58, 60 and 63°C, scaled to the known viscosities at 20 °C, and globally fitted with water $(X=0)$[48] viscosities to yield the following model equations:

$$\eta_{H_2O}(T)=0.226+1.0723^3 \ e^{-(T-10)/33} \quad \text{[3a]}$$

$$\eta_{Ficoll}(T,X)=(1+0.3843X-0.00508X^2)^3 \\ [1+(1.966+0.234X)e^{-0.0235T}-(1.275-0.0283X)e^{-0.0036T}] \quad \text{, [3b]}$$

where *T* is in °C, *X* is in mg/ml (mass of crowder/total solution volume), and   is the viscosity in centiPoise units.

3. Results

3.1 Crowding effect of Ficoll 70 on λ₆₋₈₅ stability

The 70 kDa carbohydrate polymer Ficoll 70 acts as a $\approx$5.1 nm Stokes radius semi-rigid crowding agent in aqueous solution. We studied the stability of λ^*_{6-85} YG (9.2 kDa, hydrated radius of gyration *ca.* 1.2 nm [49]) in a Ficoll crowding matrix of volume fraction $\varphi \approx$15–16% in phosphate buffer at pH 7. A Trp22-Tyr33 interaction acts as a probe of non-local tertiary contact formation in λ^*_{6-85} YG.[23]

The melting point obtained by circular dichroism (CD) is T_m=54±1 °C in Ficoll, identical within measurement uncertainty with T_m=55±1 °C in buffer, which agrees with the previous literature value of 54.5 °C.[42] Furthermore, the cooperativity parameter $C^{(1)}$ from eq. [2] was 502±28 J mol^{-1} K^{-1} in Ficoll and 521±39 J mol^{-1} K^{-1} in buffer. Thus concentrations of over 200 mg/ml of Ficoll 70 have no appreciable effect on thermal stability of lambda repressor secondary structure compared to buffer. Ficoll does affect the shape of the CD spectrum, with more random coil signal (deeper peak at 208 nm relative to 222 nm [50]) than in aqueous buffer (Figure 2A inset).

The fluorescence intensity probe reveals a larger difference between Ficoll crowding and aqueous buffer (Figure 2B): T_m remains 54±1 °C in φ=15% Ficoll, but it decreases to 49 °C in aqueous buffer. This difference between CD and fluorescence probes has been observed before for other lambda repressor fragment mutants,[15, 51] and is a signature for deviations from two-state folding over a single barrier. Thus thermal stabilization of λ^*_{6-85} YG by 225–240 mg/ml Ficoll is in the range of −1 to 5 °C, depending on the probe.

We also carried out measurements in sucrose for reference, and obtained melting points of 54 and 51 °C by CD and fluorescence. Sucrose occupies an intermediate ground between aqueous buffer and Ficoll, also not strongly stabilizing λ^*_{6-85} YG relative to aqueous buffer.

3.2 Folding relaxation kinetics of $\lambda_{6\text{-}85}$ in Ficoll 70

We investigated the folding kinetics of λ_{6-85}^* YG to see if a larger kinetic effect could be obtained. Temperature jump relaxation rates k_{obs} were measured around T_m, between 47 and 60 °C final temperatures. Representative jumps to a final temperature of 54 °C are shown in Figure 3A in aqueous buffer, φ=15% sucrose and φ=15% Ficoll. An Arrhenius plot of the observed relaxation rate is shown in Figure 3B. The buffer, Ficoll, and sucrose reference data differ by less than 0.2 natural log units, or 20% of the rate.

To compare folding rates further, we made the two-state approximation $k_{obs} \approx k_a + k_d/K_{eq} = k_a(K_{eq}+1)/K_{eq}$ and scaled the folding rate coefficient k_a by $(T)^{-1}$. (We used the equilibrium constant K_{eq} from the fluorescence data in 3.2 because fluorescence was used to detect the kinetics.) The result is shown in Figure 3B for an average over several data sets taken with φ=10–15% Ficoll *vs.* 0% (buffer). The estimated activated folding rates in buffer and Ficoll are virtually identical over the temperature range we covered. Ficoll neither greatly stabilizes λ_{6-85}^* YG, nor does it increase the folding rate significantly.

As seen in Figure 3A, sucrose and Ficoll have a very fast phase with rate coefficient $k_m \approx (2 \text{ μs})^{-1}$. A small fast phase is observed in sucrose, and a significantly larger one in Ficoll, even though the main folding rate coefficient k_a does not speed up appreciably in sucrose and Ficoll. Such phases have been observed for downhill-folding lambda repressor mutants with experimental and calculated barriers < 7 kJ/mole.[11, 15] The 'burst' with rate coefficient k_m is not observed for λ_{6-85}^* YG in aqueous buffer, in agreement with previous studies.[47]

3.3 High stability and low background fluorescence of SubL for crowding studies

With Ficoll having a relatively modest effect, we wanted to see if the crowding matrix/$_{6\text{-}85}$ combination could be optimized to produce large signals and large T_m changes in a small, fast folder like lambda repressor fragment. A small protein could act as a more compact crowding agent, predicted to have a larger effect by excluded volume models.[52] We chose as our matrix candidate the 14 kDa thermophilic protein SubL, the L subunit of an archaeal DNA repair protein.[41] As the probe protein, we investigated λ_{6-85}^*, which has a fluorescence-detected thermal stability similar to λ_{6-85}^* YG, but a strongly decreasing fluorescence signal as it unfolds, easy to detect in a slightly fluorescent matrix.

To be suitable as a crowding agent for fluorescence-detected thermal melts, a protein must be easy to purify in large quantities, must be highly thermostable even at high concentration, and must fluoresce as little as possible (Figure 4). A thermal scan of SubL circular dichroism shows no evidence of unfolding at temperatures below 70 °C. The magnitude of the CD_{222} spectrum increases with temperature (Figure 4B), indicating more secondary structure at high temperature. Thus SubL has a much higher melting point than λ_{6-85}^*. Only a combination of 2 molar guanidine and pH 4.5 shows evidence of unfolding beginning below 70 °C. Heating above 70 °C is required before SubL or SubL-$_{6\text{-}85}$ mixtures show strong scattering (milky solution) due to precipitation.

SubL fluorescence excited at 290 nm is approximately 60 times lower than tryptophan fluorescence from λ_{6-85}^* (Figure 4A). The small amount of residual fluorescence comes from two tyrosines, and decreases slowly with increasing temperature. Thus SubL contributes less than 14% background fluorescence in experiments with a 1:10 ratio of λ_{6-85}^* to crowder. SubL expresses in large quantities, and is easily purified by heating, whereupon only the thermophilic SubL remains in solution (see Methods).

3.4 Stabilization of $\lambda_{6\text{-}85}$ by the SubL matrix

In buffer at pH 7, λ^*_{6-85} had a melting temperature of 50±1 °C detected by total fluorescence intensity (Figure 5). Fluorescence wavelength shift (Figure 5A) yielded a slightly lower temperature, 48.5±1.5 °C. Both of these are lower than the previously measured T_m detected by circular dichroism,[42] indicating a deviation from a simple two-state equilibrium.

We investigated the effect of crowding on the thermal stability of λ^*_{6-85} at matrix concentrations φ = 14% ($\approx$220 mg/ml SubL), similar to the Ficoll concentrations in sections 3.1–3.2 (Figure 5B). Fluorescence spectra were obtained at 1 nm wavelength intervals and at 5 °C temperature intervals to minimize heating time and aggregation during thermal denaturation. The thermodynamic fit yielded T_m = 63±2 °C, which is 13 °C higher than the T_m = 50 °C measured in buffer. The cooperativity in SubL was not appreciably different from buffer, and was globally fitted to $C^{(1)}$ = 124±30 J mol^{-1} K^{-1}. A similar analysis by wavelength shift (Figure 5A) yielded the same $C^{(1)}$ and a smaller change of T_m between buffer and matrix (7 °C), but still larger than obtained in Ficoll. We could not compare fluorescence and CD probes in SubL because of the large CD signal from the SubL crowding matrix.

4. Discussion

The stability of several proteins has been investigated in Ficoll or similar synthetic crowding matrices, notably apoflavodoxin,[33, 37] VlSE,[33] PGK[44] and on the small size end, cytochrome c.[40] The consensus is that synthetic crowders enhance the stability of relatively large proteins. Some proteinaceous crowding matrices, such as lysozyme, have been shown to destabilize probe proteins.[36] Thus there is room for both excluded volume effects (stabilizing), and other effects (e.g. destabilizing electrostatics) of the crowding matrix.

Here we find that SubL acts as a strongly stabilizing matrix for the small protein λ^*_{6-85}, whereas the 5 times larger (by mass) Ficoll 70 acts only as a modest stabilizing agent at the same crowding fraction (φ=14–16%). It is thus possible for protein crowding matrices to stabilize probe proteins even more so than a synthetic crowding matrix. Indeed, experiments in live cells, where proteins are expected to be important crowding agents, have also shown that probe proteins are stabilized.[39, 53]

Simple models that emphasize excluded volume have been developed.[52, 54, 55] In these models, rigid globular crowders act by restricting the configurational entropy of the probe protein's denatured ensemble. Thereby they destabilize the denatured state and speed up refolding except at the very highest crowder concentrations. Cheung and Thirumalai predict how T_m increases with crowder volume fraction φ_c, assuming a random coil denatured state:

$$\Delta T_m \approx 0.84 \cdot T_m(\text{Kelvin}) \cdot \phi_c^{1.8} \quad [4]$$

The general trend is consistent with lysozyme in dextran matrices[56] and PGK in Ficoll matrix,[44] for example.

Of the two cases studied here, eq. [4] adequately describes the temperature shift observed for λ^*_{6-85} in the SubL matrix: we measure an average of 10 °C by two different fluorescence methods (intensity, wavelength), compared to eq. [4] predicting 8 °C for λ^*_{6-85} in 14% crowder. Of course, this agreement indicates only that excluded volume effects can account for the observed order of magnitude of the T change: λ^*_{6-85} in SubL has probe-dependent melting temperatures with a 6 °C range (indicating breakdown of the two-state assumption).

The predictions of simple crowding models generally break down for λ_{6-85}^* YG in Ficoll 70: Protein stability is enhanced by at most half the prediction of eq. [4], and the folding rate does not speed up at all. The most likely reason for the breakdown is the size difference between protein and crowding agent. Minton's excluded volume models predict that crowding effects increase for smaller matrix constituents, as observed here for Ficoll *vs.* SubL.[52] (Of course, this can hold only up to a point: if the carbohydrate crowder is made very small compared to the probe protein, e.g. sucrose compared to λ_{6-85}^* YG, it must act like a cosmotrope rather than a crowding agent.) Ficoll 70 may simply be too large to efficiently crowd λ_{6-85}^* YG. In addition, the highly hydrated, low density Ficoll molecule is likely to be softer and more penetrable than the dense (ca. 1.5 g/ml) SubL, further reducing its ability to conformationally restrict the dynamics of the small lambda repressor fragment unfolded state.

A model for Ficoll 70 crowding of λ_{6-85}^* YG must explain the following four observations: 1) secondary structure is not stabilized by crowding (CD data); 2) non-local tertiary contacts are stabilized slightly by crowding (Y33-W22 probe[23]); 3) the activated folding rate is not altered by crowding; 4) a new fast phase appears, so crowding favors downhill folding. The following hypothesis accounts for all of these: Ficoll 70 interstitial spaces have higher local viscosity than bulk water, and they are smaller than the length scale of tertiary interactions, but larger than the length scale of local secondary structure of lambda repressor fragemnt. If so, Ficoll 70 would stabilize tertiary structure more than secondary structure, and the unchanged activated rate results from a cancellation of higher local viscosity and a lower activation barrier; the lower barrier in turn causes the appearance of the fast molecular phase k_m and downhill folding. There is experimental and computational precedent showing that increased local viscosity reduces folding rates. Mukherjee *et al.* previously showed that crowding of small model peptides by Ficoll 70 can cause a slow-down of secondary structure formation.[57] In live cells, the local viscosity for folding has been shown to increase by a factor of 2 from aqueous solution,[58] so compensation of a lower barrier by higher viscosity is plausible. Ando and Skolnick calculated that local viscosity variations can result from hydrodynamics, as the drag of aqueous layers flowing past multiple macromolecules changes the local viscosity from the bulk value.[59]

In view of our results, it will be very interesting to develop improved theoretical and computational models for crowders of small fast-folding proteins. Such models should include crowder flexibility, local viscosity, hydrodynamic and electrostatic effects on the probe protein, in addition to the excluded volume effect. Small proteins like λ_{6-85}^* are ideal probes for crowding studies because they can be modeled at atomistic detail with currently available molecular dynamics technology. Computational efforts for small model proteins with rigid crowers are already underway.[40, 60] On the experimental side, it will be useful to provide systematic folding kinetics data for fast-folding small probe proteins in different crowding environments. For example, a series of λ_{6-85}^* mutants in Ficoll or SubL could pin down how protein stability, denatured state compactness, and other properties that can be varied by mutation, affect the ability of the matrix to crowd the probe protein.

Acknowledgments

References

1. Kramers HA. Physica. 1940; 7:284.

2. Homouz D, Perham M, Samiotakis A, Cheung MS, Wittung-Stafshede P. Proc Nat Acad Sci USA. 2008; 105:11754–11759. [PubMed: 18697933]

3. Lindorff-Larsen K, Piana S, Dror RO, Shaw DE. Science. 2011; 334:517–520. [PubMed: 22034434]

4. Onuchic JN, Wolynes PG, Luthey-Schulten Z, Socci ND. Proc Natl Acad Sci USA. 1995; 92:3626–3630. [PubMed: 7724609]

5. Jackson SE, Fersht AR. Biochemistry. 1991; 30:10428–10435. [PubMed: 1931967]

6. Chandler D. J Chem Phys. 1978; 68:2959–2970.

7. Sims IR, Smith IWM. Ann Rev Phys Chem. 1995; 46:109–137.

8. Sabelko J, Ervin J, Gruebele M. Proc Nat Acad Sci USA. 1999; 96:6031–6036. [PubMed: 10339536]

9. Garcia-Mira M, Sadqi M, Fischer N, Sanchez-Ruiz JM, Muñoz V. Science. 2002; 298:2191–2195. [PubMed: 12481137]

10. Cavalli A, Haberthur U, Paci E, Caflisch A. Protein Science. 2003; 12:1801–1803. [PubMed: 12876329]

11. Yang WY, Gruebele M. Nature. 2003; 423:193–197. [PubMed: 12736690]

12. Ma H, Gruebele M. Proc Nat Acad Sci USA. 2005; 102:2283–2287. [PubMed: 15699334]

13. Sadqi M, Fushman D, Munoz V. Nature. 2006; 442:317–321. [PubMed: 16799571]

14. Dyer RB. Current Opinion in Structural Biology. 2007; 17:38–47. [PubMed: 17223539]

15. Liu F, Gruebele M. J Mol Biol. 2007; 370:574–584. [PubMed: 17532338]

16. Fung A, Li P, Godoy-Ruiz R, Sanchez-Ruiz JM, Munoz V. J Am Chem Soc. 2008; 130:7489–7495. [PubMed: 18479088]

17. Naganathan AN, Munoz V. Biochemistry. 2008; 47:6752–6761. [PubMed: 18540681]

18. Cho SS, Weinkam P, Wolynes PG. Proc Nat Acad Sci USA. 2008; 105:118–123. [PubMed: 18172203]

19. Godoy-Ruiz R, Henry ER, Kubelka J, Hofrichter J, Munoz V, Sanchez-Ruiz JM, Eaton WA. J Phys Chem B. 2008; 112:5938–5949. [PubMed: 18278894]

20. Liu F, Du D, Fuller AA, Davoren J, Wipf P, Kelly J, Gruebele M. Proc Nat Acad Sci USA. 2008; 105:2369–2374. [PubMed: 18268349]

21. Pitera JW, Swope WC, Abraham FF. Biophys J. 2008; 94:4837–4846. [PubMed: 18326644]

22. DeCamp SJ, Naganathan AN, Waldauer SA, Bakajin O, Lapidus LJ. Biophysical Journal. 2009; 97:1772–1777. [PubMed: 19751683]

23. Liu F, Gao YG, Gruebele M. J Mol Biol. 2009; 397:789–798. [PubMed: 20138892]

24. Dumont C, Emilsson T, Gruebele M. Nature Methods. 2009; 6:515–519. [PubMed: 19483692]

25. Best RB, Hummer G. Proc Nat Acad Sci USA. 2005; 102:6732–6737. [PubMed: 15814618]

26. Shaw DE, Maragakis P, Lindorff-Larsen K, Piana S, Dror RO, Eastwood MP, Bank JA, Jumper JM, Salmon JK, Shan YB, Wriggers W. Science. 2010; 330:341–346. [PubMed: 20947758]

27. Ensign DL, Kasson PM, Pande VS. J of Mol Biol. 2007; 374:806–816. [PubMed: 17950314]

28. Freddolino PL, Harrison CB, Liu YX, Schulten K. Nature Physics. 2010; 6:751–758.

29. Ellis JP, Culviner PH, Cavagnero S. Protein Science. 2009; 18:2003–2015. [PubMed: 19569194]

30. Ugrinov KG, Clark PL. Biophys J. 2010; 98:1312–1320. [PubMed: 20371331]

31. Minton AP, Wilf J. Biochemistry. 1981; 20:4821–4826. [PubMed: 7295652]

32. van den Berg B, Wain R, Dobson CM, Ellis RJ. The EMBO Journal. 2000; 19:3870–3875. [PubMed: 10921869]

33. Perham M, Stagg L, Wittung-Stafshede P. FEBS Letters. 2007; 581:5065–5069. [PubMed: 17919600]

34. Samiotakis A, Wittung-Stafshede P, Cheung MS. International Journal of Molecular Sciences. 2009; 10:572–588. [PubMed: 19333422]

35. Wang Y, Li C, Pielak GJ. J Am Chem Soc. 2010; 132:9392–9397. [PubMed: 20560582]

36. Miklos AC, Sarkar M, Wang Y, Pielak GJ. J Am Chem Soc. 2011; 133:7116–7120. [PubMed: 21506571]

37. Stagg L, Christiansen A, Wittung-Stafshede P. Journal of the American Chemical Society. 2011; 133:646–648. [PubMed: 21175168]

38. Ignatova Z, Gierasch LM. Proceedings of the National Academy of Sciences of the United States of America. 2004; 101:523–528. [PubMed: 14701904]

39. Ebbinghaus S, Dhar A, McDonald JD, Gruebele M. Nat Methods. 2010; 7:319–323. [PubMed: 20190760]

40. Christiansen A, Wang Q, Samiotakis A, Cheung MS, Wittung-Stafshede P. Biochemistry. 2010; 49:6519–6530. [PubMed: 20593812]

41. Reich CI, McNeil LK, Brace JL, Brucker JK, Olsen GJ. Extremophiles. 2001; 5:265–275. [PubMed: 11523896]

42. Yang WY, Gruebele M. Biochemistry. 2004; 43:13018–13025. [PubMed: 15476395]

43. Ghaemmaghami S, Word JM, Burton RE, Richardson JS, Oas TG. Biochemistry. 1998; 37:9179–9185. [PubMed: 9636065]

44. Dhar A, Samiotakis A, Ebbinghaus S, Nienhaus L, Homouz D, Gruebele M, Cheung MS. Proc Natl Acad Sci. 2010; 107:17586–17591. [PubMed: 20921368]

45. Nishii I, Kataoka M, Tokunaga F, Goto Y. Biochemistry. 1994; 33:4903–4909. [PubMed: 8161550]

46. Ballew RM, Sabelko J, Reiner C, Gruebele M. Rev Sci Instrum. 1996; 67:3694–3699.

47. Yang W, Gruebele M. Biophys J. 2004; 87:596–608. [PubMed: 15240492]

48. Perry, RH.; Chilton, CH. Perry's Chemical Engineer's Handbook. Mc Graw-Hill; New York: 1973.

49. Kim SJ, Dumont C, Gruebele M. Biophys J. 2008; 94:4924–4931. [PubMed: 18326645]

50. Berova, N.; Nakanishi, K.; Woody, RW. Circular dichroism: principles and applications. Wiley; New York: 2000.

51. Prigozhin MB, Gruebele M. Journal of the American Chemical Society. 2011; 133:19338–19341. [PubMed: 22066714]

52. Minton AP. Biophys J. 2005; 88:971–985. [PubMed: 15596487]

53. Dhar A, Girdhar K, Singh D, Gelman H, Ebbinghaus S, Gruebele M. Biophys J. 2011; 101:421–430. [PubMed: 21767495]

54. Minton AP. Biophys J. 2000; 78:101–109. [PubMed: 10620277]

55. Cheung MS, Klimov Dmitri, Thirumalai D. Proc Nat Acad Sci USA. 2005; 102:4753–4758. [PubMed: 15781864]

56. Sasahara K, McPhie P, Minton AP. J Mol Bio. 2003; 326:1227–1237. [PubMed: 12589765]

57. Mukherjee S, Waegele MM, Chowdhury P, Guo L, Gai F. Journal of Molecular Biology. 2009; 393:227–236. [PubMed: 19682997]

58. Dhar A, Ebbinghaus S, Shen Z, Mishra T, Gruebele M. Biophys J. 2010; 99:L69–L71. [PubMed: 21044564]

59. Ando T, Skolnick J. Proc Nat Acad Sci USA. 2010; 107:18457–18462. [PubMed: 20937902]

60. Samiotakis A, Cheung MS. J Chem Phys. 2011; 135.

61. Humphrey WF, Dalke A, Schulten K. J Mol Graphics. 1996; 14:33–38.
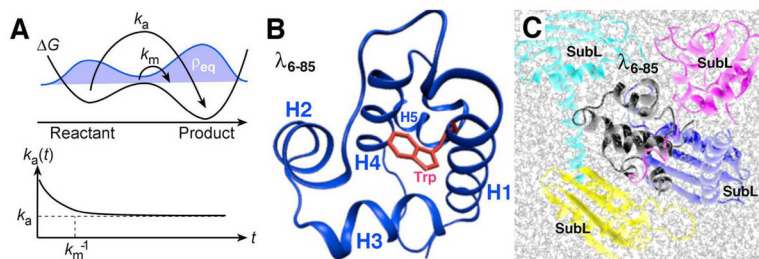
Figure 1.
(A) Connection between kinetics and dynamics. If the unimolecular activation barrier is very low (middle of ΔG curve), a measurable activated population exists (middle of the shaded equilibrium population ρ_{eq}). This population reacts by direct diffusion with a rate $k_m \gg k_a$. Thus the rate coefficient $k_a(t)$ does not immediately settle into a constant value k_a: the usual unimolecular concentration change $\sim\exp[-k_a t]$ is preceded by a short 'burst' of very fast reaction, allowing a direct independent measurement of the prefactor k_m in the equation $k_a = k_m \exp[-\Delta G^{\dagger}/RT]$ for the activated rate coefficient k_a. The size of the short burst is proportional to the activated population, and becomes unobservable when the activation barrier is very high. (B) Monomer of lambda repressor fragment 6–85 showing the tryptophan fluorescence probe as a stick structure, and helices 1 through 5 as ribbon structures. (C) Model of $\lambda_{6\text{-}85}$ in 200 mg/ml SubL, to indicate the nature of the crowding effect. Water molecules are shown as small gray sticks. Plots were created using the free visualization software VMD.[61]
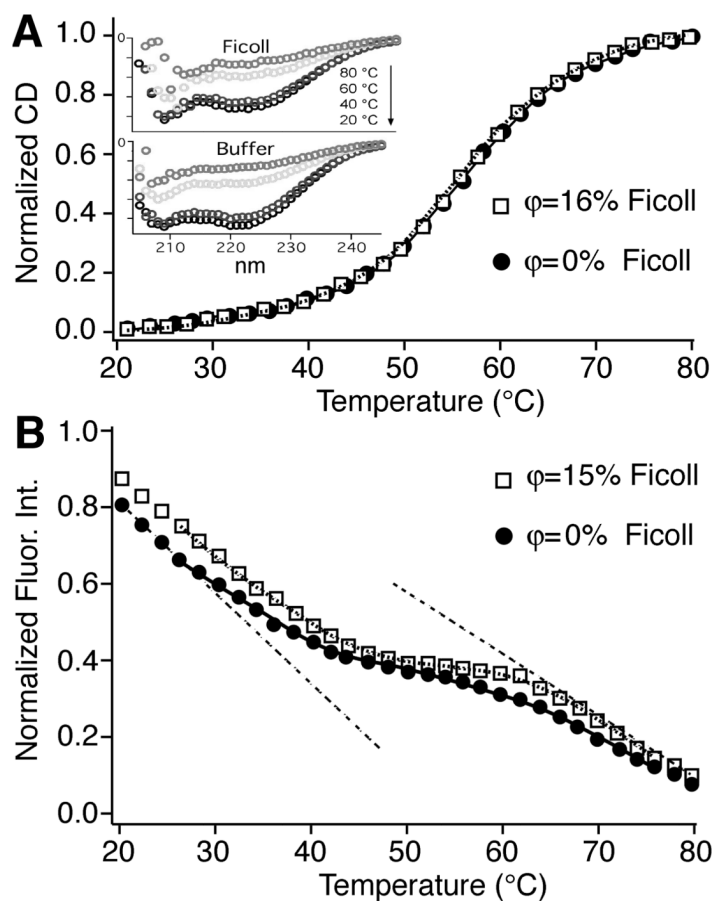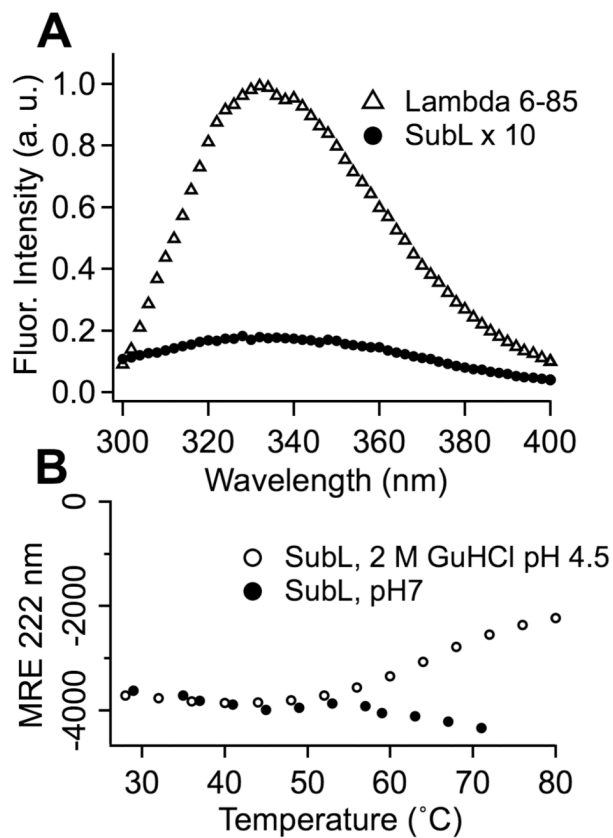
Figure 2.
Stability of λ^*_{6-85} Q33Y in aqueous buffer and Ficoll. Protein concentration was 7.1–7.2 μM for the protein in Ficoll, and 7.2 μM for protein in buffer (50 mM phosphate buffer at pH 7). Markers are measured, solid and dotted curves are fits to equation [2] (A) Circular dichroism-detected thermal melts with 240 mg/ml Ficoll and without Ficoll. The insets show the CD spectra at 4 temperatures, indicating more random coil structure in Ficoll (scale 0 top to −30,000 bottom MRE in ° cm^2 dmol^{-1} residue^{-1}). (B) Fluorescence intensity-detected thermal melt of λ^*_{6-85} Q33Y with 225 mg/ml Ficoll and in buffer (50 mM phosphate buffer at pH 7). The dashed lines are two of the four fitted baselines. Melting temperatures given in the text were extracted by fitting to eq. [2].
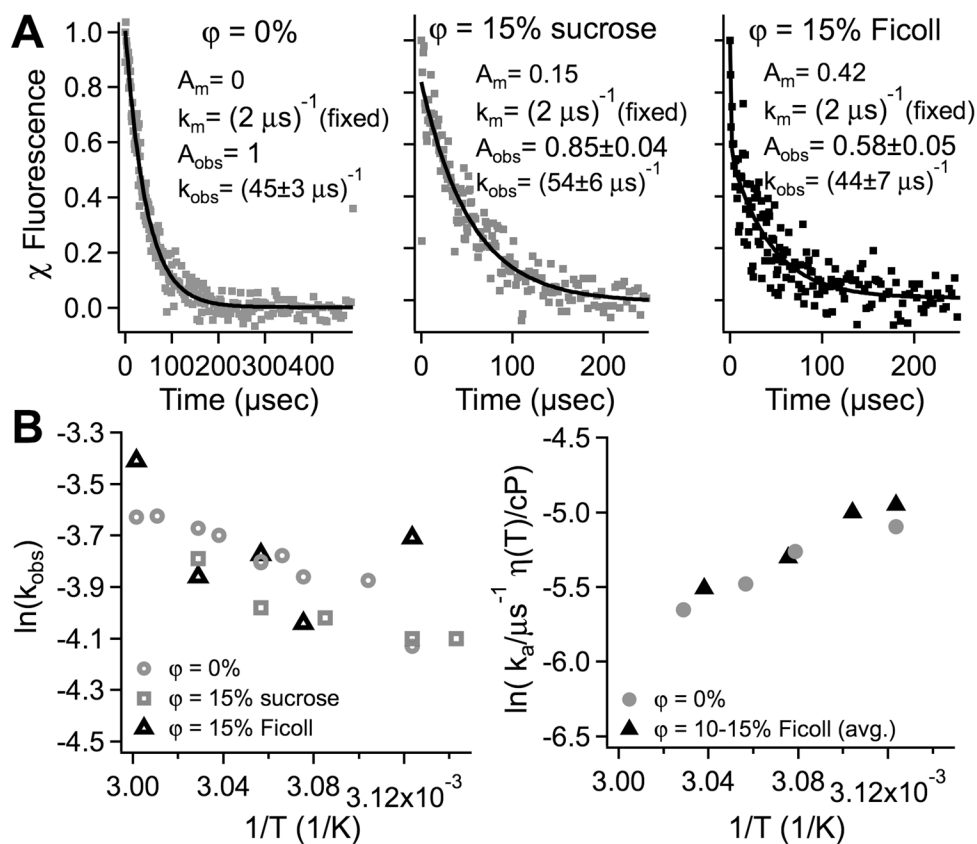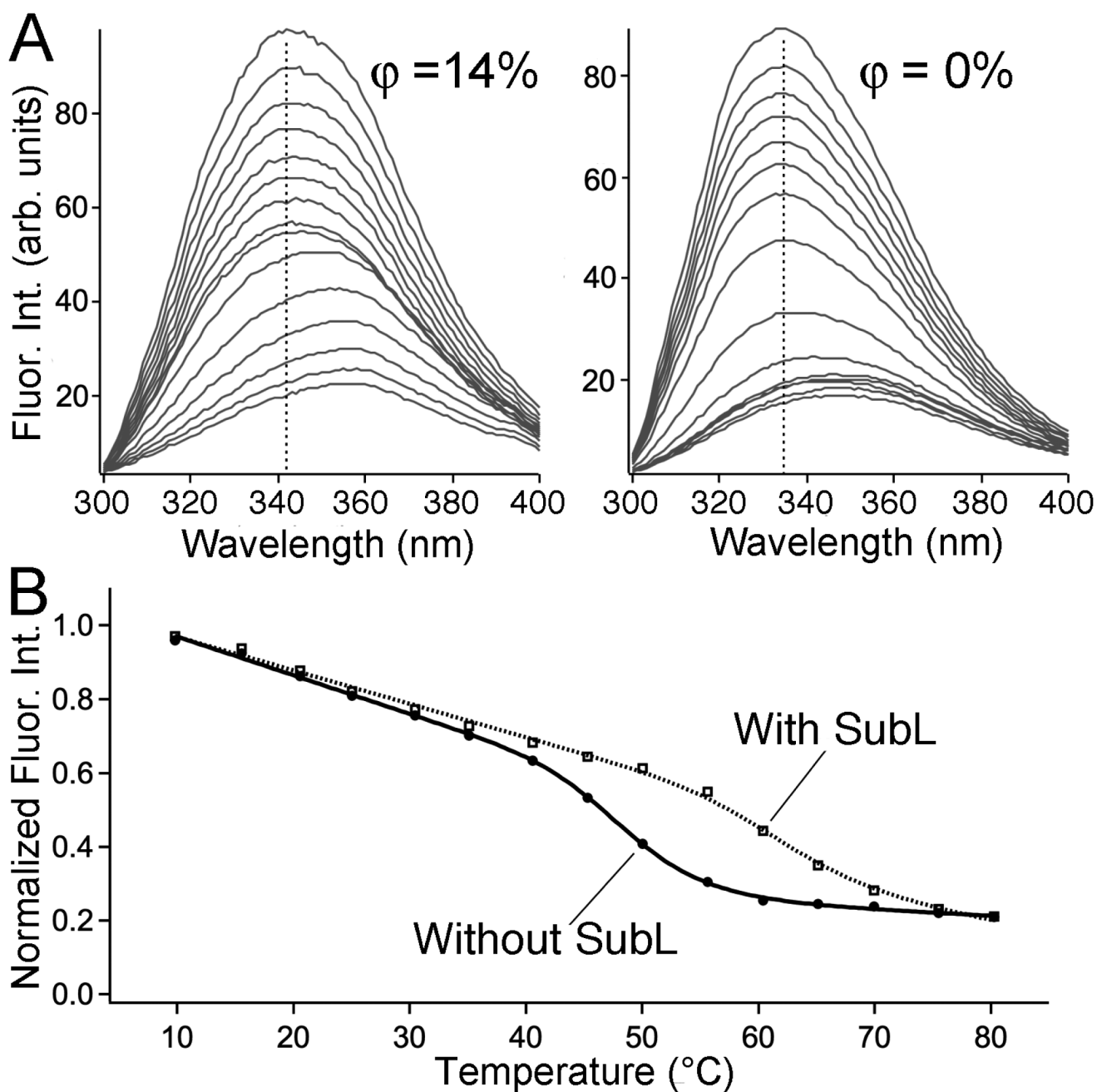
Figure 3.
Temperature jump relaxation kinetics of λ^*_{6-85} Q33Y in aqueous buffer, sucrose and Ficoll.
(A) 6±1 °C T-jumps of 83 μM protein to a final temperature of 54 °C. Data are shown as
dots, fits to a double exponential (rate coefficients k_m and $k_{obs} = k_a + k_d/K_{eq}$) as black lines.
The molecular phase k_m (rapid 'burst' of diffusing transition state population) tends to be
larger in sucrose and Ficoll jumps. (B) Arrhenius plots of the fitted rate coefficients k_{obs},
and of the viscosity-scaled activated folding rate k_a as described in the text. No significant
deviations between Ficoll and aqueous buffer (50 mM phosphate buffer at pH 7) are seen.

Figure 4.
Fluorescence and stability of SubL. (A) Peak SubL fluorescence is *ca.* 60 times smaller than peak λ^*_{6-85} fluorescence at the same concentration (normalized to 100 μM). (B) Thermophilic SubL at pH 7 shows no evidence of melting below 70 °C, as determined by circular dichroism Mean Residue Ellipticity (MRE in ° cm^2 $dmol^{-1}$ $residue^{-1}$). Only in acidic guanidinium solution was there any evidence of unfolding below 70 °C (at ca. 55 °C).

Figure 5.
(A) 12 mg/ml λ^*_{6-85} in 220 mg/ml SubL (left), and 12 mg/ml λ^*_{6-85} in buffer only (right) fluorescence spectra. Temperatures are (in order of decreasing intensity, ±1 °C absolute calibration): 10 to 80 °C, in 5 °C steps. The decrease of total fluorescence intensity, as well as the red-shift of the peak wavelength from the folded reference wavelength (vertical dashed line) can be seen clearly. (B) Integrated fluorescence intensity as a function of temperature, showing the melting transitions with and without the SubL crowding matrix.